LA-UR-80-2445

TITLE: A NUMERICAL STUDY OF THE NOL LARGE-SCALE GAP TEST

AUTHOR(S): Allen L. Bowman

SUBMITTED TO: Chemical Propulsion Information Agency

MASTER

University of California

LOS ALAMOS SCIENTIFIC LABORATORY
Post Office Box 1663 Los Alamos, New Mexico 87545
An Affirmative Action/Equal Opportunity Employer

UNCLASSIFIED

A NUMERICAL STUDY OF THE NOL LARGE-SCALE GAP TEST*

Allen L. Bowman
Los Alamos Scientific Laboratory
Los Alamos, New Mexico

ABSTRACT

The NOL large-scale gap test has been modeled numerically using the LASL reactive hydrodynamics code 2DE with Forest Fire burn rates. The model gives good agreement between calculated and experimental critical gap values for VTQ-2 and Composition B. The calibration of peak pressure in the gap versus gap length has been obtained from these calculations, and is in good agreement with the published experimental curve. The two-dimensional nature of the gap test is evident from the curvature of the shock wave in the gap and test sample, and from the observed distance of run to detonation in the test samples.

INTRODUCTION

The relative shock sensitivities of explosive compositions are commonly assessed by means of gap tests. In these tests the shock from a standard donor explosive is transmitted to the test explosive through an inert barrier (gap). The shock sensitivity of the test material is characterized by the gap thickness for which the probability of detonation is 0.5. Hercules Inc. is using the NOL** large-scale gap test[1] as a means of evaluating the effects of rocket propellant formulation and processing variables on the reaction of the propellant to shock. This test has been modeled numerically to provide a better understanding of the details of the processes involved.

EXPERIMENT AND MODEL

The experimental arrangement of the NOL gap test is shown in Fig. 1. A J-2 blasting cap (Hercules) is used to initiate the standard donor, which is two pressed pentolite pellets, 2-in. diameter by 1-in. long, with density of 1.56 g/cm^3. The gap is made up of Plexiglas (polymethyl methacrylate) disks of 2-in. diameter. The test explosive is formed to fit a seamless steel tube of 5.6-mm wall thickness. A 9.5-mm-thick mild steel witness plate is used. A "go" result is defined by a clean hole punched in the plate. The test procedure is a modification of the Bruceton up-and-down technique.

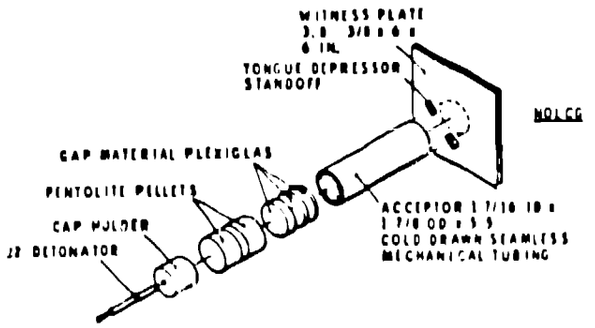

Figure 1. NOL large-scale gap test configuration.

The computation of gap test behavior was performed with the

*Work performed under Contract N0003079 MD 790009 SSPO 13, Task 1.
**Naval Ordnance Laboratory, White Oak, now Naval Surface Weapons Center, Silver Spring, MD.
Approved for public release; distribution unlimited.

UNCLASSIFIED

two-dimensional reactive hydrodynamic code 2DE[2,3] using the Forest Fire burn rate[2,4] for the test sample and the C-J volume burn model[2] for the pentolite donor. The test was modeled at its true dimensions, using a 1.826-mm cell dimension. The model geometry is shown in Fig. 2. An unconfined test calculation was made with the same model, with the steel tube replaced by air. The donor explosive was initiated by a hot spot of 3.7-mm radius and length to model the effect of the J-2 cap. The hot spot is fully reacted explosive (gaseous products) with density and energy initialized to isentrope conditions at ∿ 1.02 x C-J pressure.

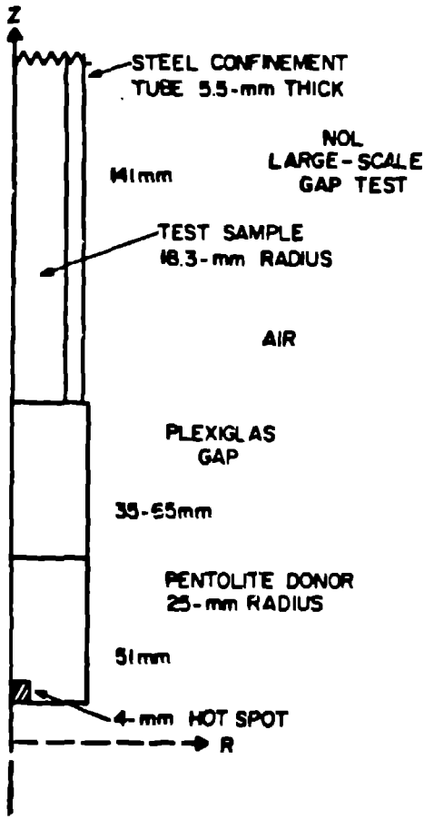

Figure 2. NOL gap test model. The symmetry axis of the cylindrical assembly is at the left of this model. The initiation of the donor is modeled by a hot spot of 3.7-mm radius and length.

RESULTS AND DISCUSSION

The detonation behavior of the donor cylinder is shown in Fig. 3 by a series of contour plots of mass fraction and density. The mass fraction W is defined such that W = 1 for a solid and W = 0 for a gas, with a continuous variation between these limits for a burning explosive. The strongly divergent detonation wave builds slowly to a pressure of 14.5 GPa, which is much less than the C-J pressure of 22.8 GPa obtained from a BKW calculation.[5] The calculated particle velocity (U_p) at the detonation front is 1.15 mm/μs and the detonation velocity is 7.5 mm/μs.

The initial shock pressure in the gap is obtained graphically as the intersection of the isentrope of the pentolite detonation products with the Plexiglas Hugoniot. These curves are shown in the pressure-particle velocity plane in Fig. 4. The intersection point, shown as a square, gives an induced pressure of 10.3 GPa. The isentrope is run through the point (p = 14.5, U_p = 1.15) obtained from these calculations for pentolite. This point is indicated by a circle in Fig. 4. The peak pressures that are developed in the Plexiglas gap by the passage of the shock wave are readily obtained from these calculations. This permits the construction of a calibration curve of gap pressure versus gap thickness, which is compared with an experimental calibration[6] in Fig. 5. The high pressures at small gap (<10 mm) are not experimental values, but are based on a zero gap value derived from the graphical matching described above, using the assumption of C-J pressure

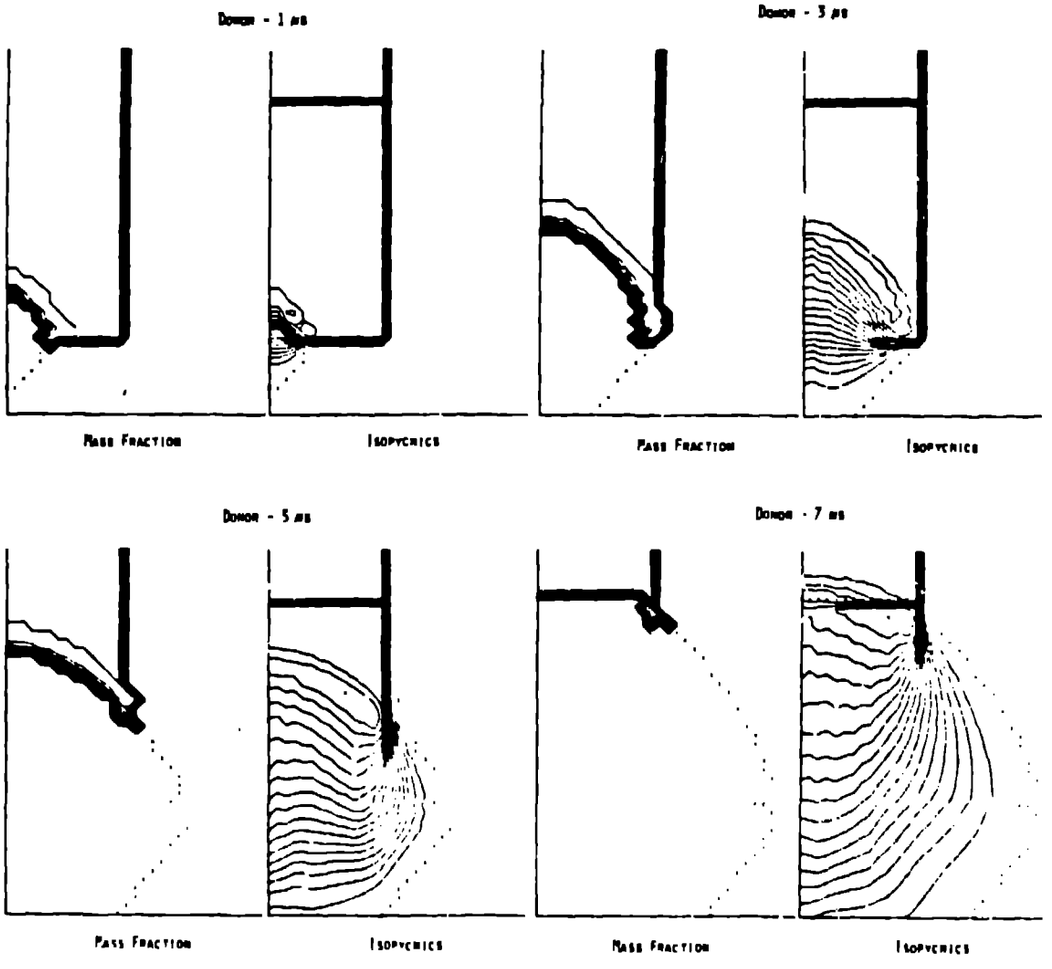

Figure 3. Detonation of the NOL gap test donor. Pentolite cylinder, 25-mm radius by 51 mm long, at 1, 3, 5, and 7 μs. Contour plots of mass fraction (0.05 interval) and density (0.1 g/cm^3 interval). The shock has entered the Plexiglas gap at 7 μs.

in the pentolite.* The experimental and calculated curves agree within their uncertainties for gap thicknesses greater than 10 mm. The calculated curve will be used for all further discussion.

The NOL large-scale gap test was run with VTQ-2 and Composition B as test explosives. The VTQ-2 was also run without the steel tube to study

*This assumption is not correct. It has been shown from theoretical arguments that the Rankine-Hugoniot equations and the Chapman-Jouguet condition are not appropriate to the description of a "steady" diverging cylindrical or spherical detonation wave.[7] Taylor also concluded from simpler considerations that the C-J pressure may not be attained although the C-J detonation velocity will be realized in a spherical wave.[8] This position is also supported by experiment (Ref. 2, pp. 116-221).

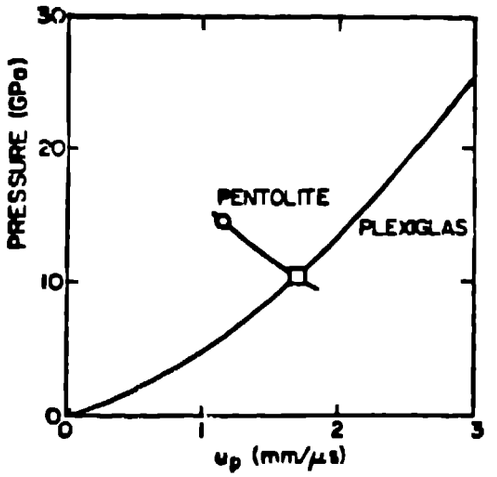

Figure 4. Impedance match at donor-gap interface. The intersection of the isentrope through the detonation state (pressure-particle velocity) with the Plexiglas Hugoniot defines the initial pressure in the gap.

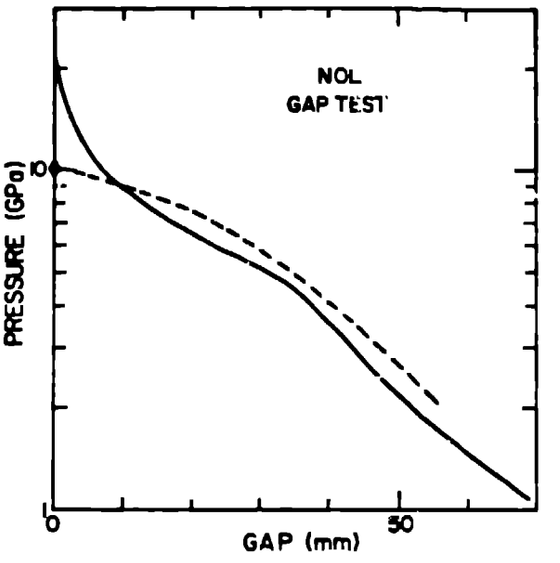

Figure 5. NOL large-scale gap test. Shock pressure in the Plexiglas gap. The solid curve is from an experimental calibration for gap lengths greater than 10 mm (Ref. 6). The dashed curve is from this study.

the effect of confinement. The results of these calculations are summarized in Table I. The pressure in the Plexiglas gap when the shock wave hits the test sample (P_g) is taken from the calibration curve (Fig. 5). The pressure induced in the sample (P_i) by this shock is obtained from a graphical impedance match. The calculated P_i is estimated from the early shock peaks in the test sample with an uncertainty of ~5%. The difference between the two values of P_i is due entirely to the effect of shock-induced chemical reaction in the test explosive. This was confirmed by performing the calculation with a nonreactive sample (same material, but with no chemical reaction permitted) of VTQ-2. The value of P_i obtained in this manner was 5.2 GPa at a 40.2 mm gap, in excellent agreement with the value of 5.3 GPa obtained from the impedance match. The detonation of VTQ-2 at a 40.2-mm gap is shown in Fig. 6 with a series of mass fraction contour plots. The shock wave enters the sample between 16 and 17 μs after the start of the run. Significant reaction is observed at 18 μs, and the partially reacted zone spreads behind the shock front, with detonation observed at 25 μs. The general behavior of the shock wave is shown by isopycnic contour plots in Fig. 7. The shock front is curved when it enters the sample at ~17 μs, and is significantly stronger on the axis. This is changed by the steel confinement tube, and by 20 μs the built-up shock wave is stronger at the tube wall, leading to detonation at the wall, rather than in the center. The detonation of VTQ-2 at a 36.5-mm gap without the steel confinement tube is shown in Figs. 8 and 9. In the absence of the supporting tube wall the curvature of the shock front increases, giving a limited zone of partial reaction, and leading to detonation in the center of the sample at 26 μs.

TABLE I

NOL LARGE-SCALE GAP TEST

	VTQ-2			Composition B				
Gap (mm)	36.6	40.2	43.8	47.5	51.1	54.8	58.4	62.1
(in.)	1.44	1.58	1.73	1.87	2.01	2.16	2.30	2.44
Pressures (GPa)								
Plexiglas gap[a]	4.7	4.0	3.4	2.9	2.5	2.2	1.9	1.6
Induced in sample:								
Calculation	8.0	6.5	5.3	4.5	3.8	3.3	2.7	2.3
Impedance match	6.1	5.2	4.3	3.5	3.1	2.7	2.3	1.9
Run distance (mm)								
Pop plot	6	8	11	15	17	20	24	29
Calculation	11	22	--	19	27	40	69	--
Transit time (μs)	24	26						
Experimental 50% gap (in.)		1.60			2.01 - 2.18			
No confinement								
Run distance (calc.)	33	--						
Experimental 50% gap		1.50						

[a]Pressures from the calibration curve, Fig. 5.

The expected length of run to detonation (χ^*) in the test sample is determined from the Pop plot using the value of P_i obtained from the impedance match. The Pop plots used in this work are shown in Fig. 10. The actual χ^* obtained from these calculations is found to be significantly longer than the expected value for gap lengths near the critical point (the maximum gap length for which detonation is observed). The data in Table I show that the ratio χ^*(calc.)/χ^*(Pop plot) reaches a value of approximately three near the critical gap length, but is probably one at much shorter gap lengths. This difference is attributed to the very nonplanar nature of the shock wave entering the test sample, as seen from Fig. 7. This is in contrast with the plane-wave one-dimensional wedge shots from which the Pop plot is determined.

CONCLUSIONS

The NOL large-scale (standard) gap test has been modeled successfully using the 2DE reactive hydrodynamic code with Forest Fire burn rates. The results of the calculations are in good agreement with experimental values. The calibration of peak pressure in the gap (P_g) versus gap length (χ) has been obtained from these calculations, and is in good agreement with the experimental curve. The distances of run to detonation obtained from these calculations are plotted versus induced pressures in Fig. 10 for comparison with the Pop plots obtained from wedge shots. The run distances

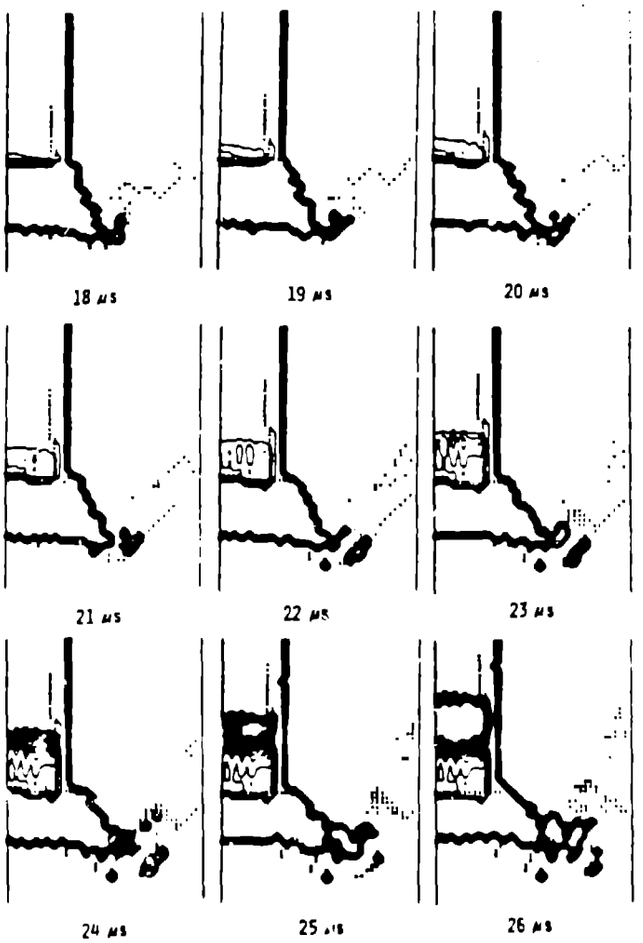

Figure 6. NOL gap test. Detonation of VTQ-2 at a 40.2-mm gap. Mass fraction contour plots.

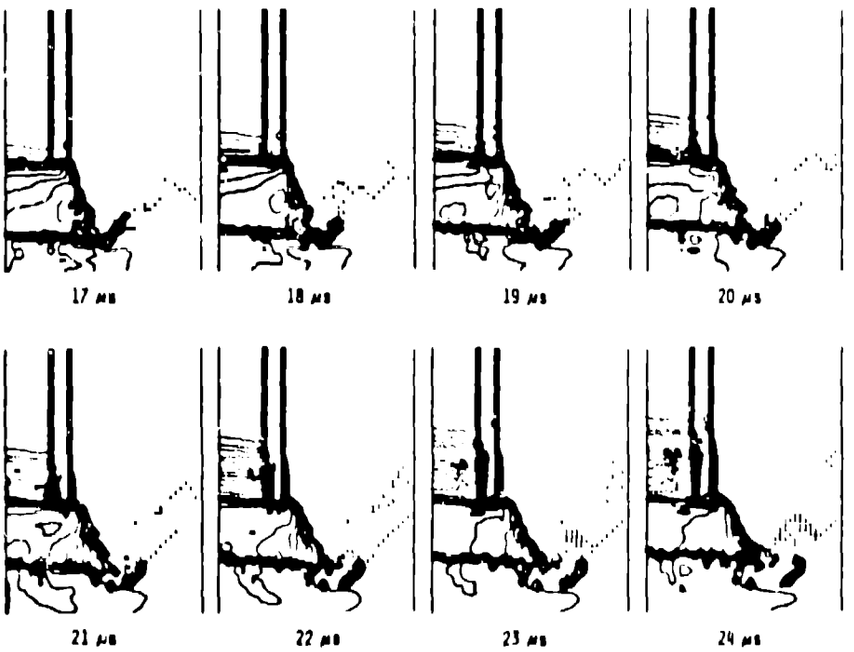

Figure 7. NOL gap test. Shock wave in VTQ-2 at a 40.2-mm gap. Isopycnic contour plots (0.1-g/cm^3 interval).

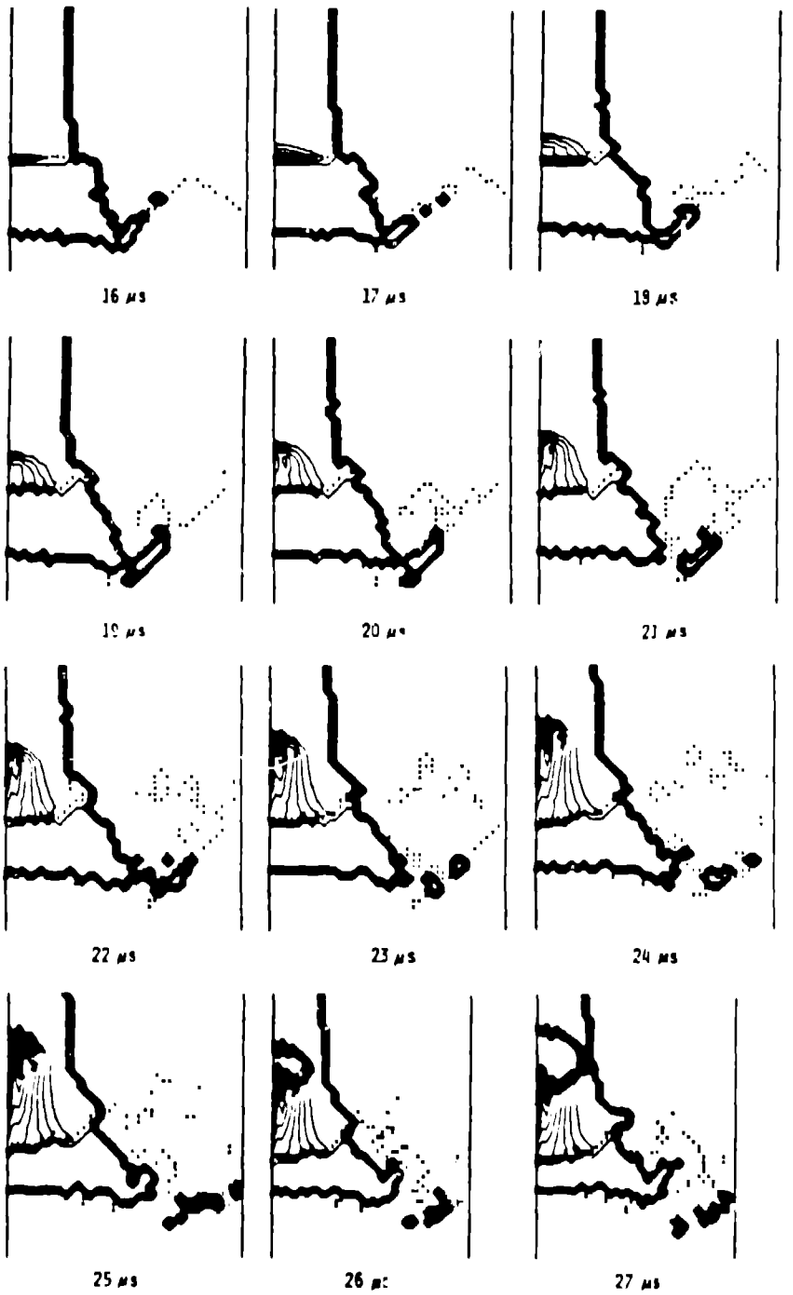

Figure 8. NOL gap test without the steel confinement tube. Detonation of VTQ-2 at a 36.5-mm gap. Mass fraction contour plots.

from the gap tests are significantly longer than those from the wedge shots at induced pressures near the critical gap length, but they approach each other at higher pressures. The critical run distance, i.e., the observed run distance at the critical gap length, increases with increasing gap length.

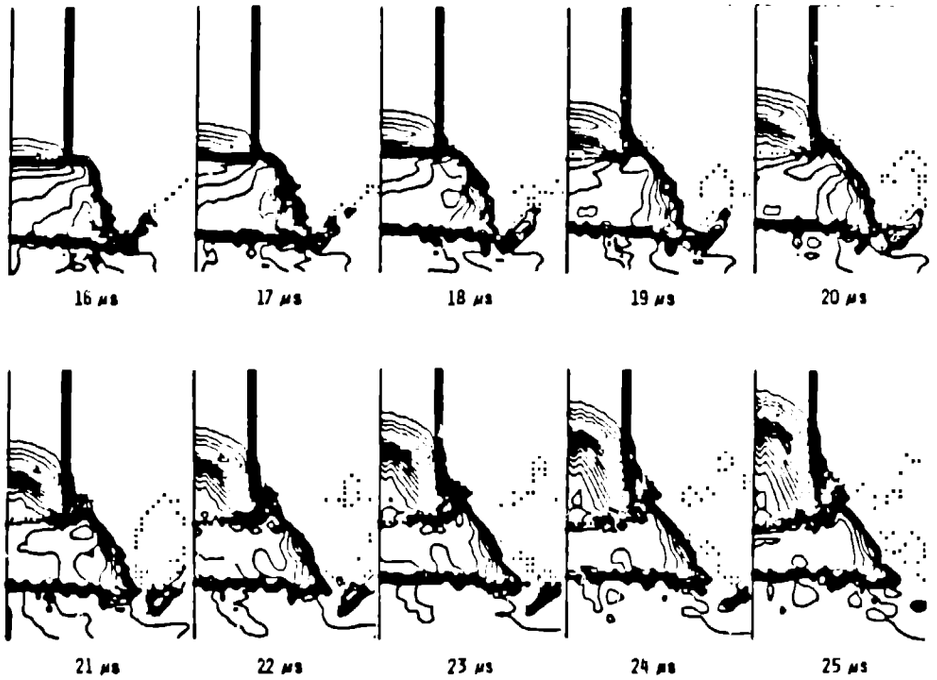

Figure 9. NOL gap test without the steel confinement tube. Shock wave in VTQ-2 at a 36.5-mm gap. Isopycnic contour plots (0.1-g/cm^3 interval).

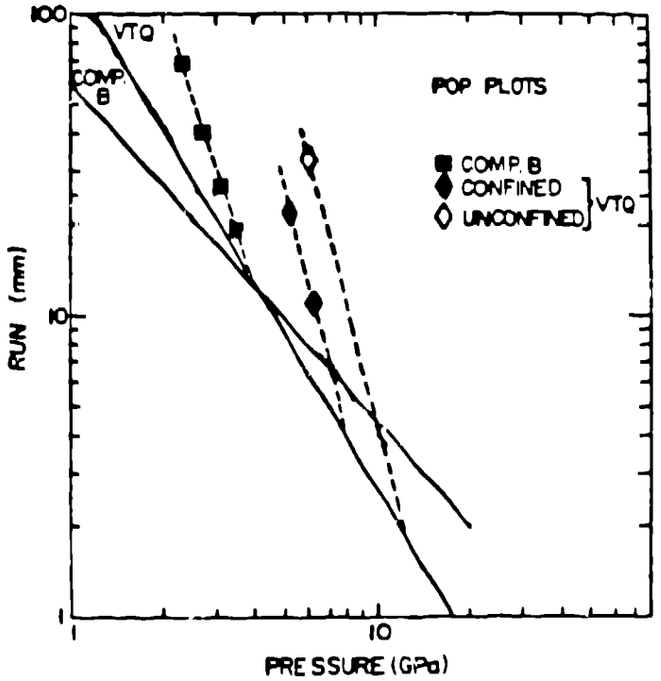

Figure 10. Pop plots of the test materials of this study, shown by solid lines. The run-pressure points obtained from this study are plotted with dotted lines to indicate approximate two-dimensional "Pop plots" defined by the gap test.

REFERENCES

1. Donna Price, A. R. Clairmont, Jr., and J. O. Erkman, "The NOL Large Scale Gap Test. III. Compilation of Unclassified Data and Supplementary Information for Interpretation of Results," NOLTR 74-40, Naval Ordnance Laboratory, Silver Spring, MD (March 1974).

2. C. L. Mader, Numerical Modeling of Detonations (University of California Press, Berkeley, 1979).

3. J. D. Kershner and C. L. Mader, "2DE, A Two-Dimensional Continuous Eulerian Hydrodynamic Code for Computing Multicomponent Reactive Hydrodynamic Problems," Los Alamos Scientific Laboratory report LA-4846 (March 1972).

4. C. L. Mader and C. A. Forest, "Two-Dimensional Homogeneous and Heterogeneous Detonation Wave Propagations," Los Alamos Scientific Laboratory report LA-6259 (June 1976).

5. C. L. Mader, "FORTRAN BKW: A Code for Computing the Detonation Properties of Explosives," Los Alamos Scientific Laboratory report LA-3704 (July 1967).

6. J. O. Erkman, D. J. Edwards, A. R. Clairmont, Jr., and Donna Price, "Calibration of the NOL Large Scale Gap Test: Hugoniot Data for Polymethyl Methacrylate," NOLTR 73-15, Naval Ordnance Laboratory, Silver Spring, MD (April 1973).

7. R. Chéret, "Theoretical Considerations on the Propagation of Shock and Detonation Waves," Fourth International Symposium on Detonation, ACR-126, 78 (1965).

8. G. Taylor, "The dynamics of the combustion products behind plane and spherical detonation fronts in explosives," Proc. Roy. Soc. A200, 235 (1950).